Electron Transport and Upper Critical Magnetic Field of $K_{1-x}Fe_{2-y}Se_2$ and $Eu_{0.5}K_{0.5}Fe_2As_2$ superconductors

V.A. Gasparov[1], A. Audouard[2], L. Drigo[2], A.I. Rodigin[3], D.L. Sun[4], C.T. Lin[4], S.L. Bud'ko[5], P.C. Canfield[5], S. Arsenijevic[6], L. Forro[6], H.S. Jeevan[7], J. Maiwald[7], P. Gegenwart[7], M. Zhang[8], A.F. Wang[8], X.H. Chen[8], V. Tsurkan[9], and J. Wosnitza[10]

1 Institute of Solid State Physics RAS, Chernogolovka, 142432, ***Russian Federation;***
2 Laboratoire National des Champs Magnétiques Intenses, Toulouse, ***France;***
3 Lomonosov Moscow State University, Moscow, ***Russian Federation****;*
4 Max Planck Institute for Solid State Research, 70569 Stuttgart, ***Germany;***
5 Ames Laboratory and Department of Physics & Astronomy, Iowa State Univ., ***USA;***
6 École Polytechnique Fédérale de Lausanne, Lausanne, ***Switzerland;***
7 I. Physik. Institut, Georg-August-Universit¨at G¨ottingen, ***Germany;***
8 Hefei National Laboratory for Physical Science at Microscale, ***China;***
9 Experimental Physics V, University of Augsburg, 86159 Augsburg, ***Germany***
10 Hochfeld-Magnetlabor Dresden (HLD), Forschungszentrum Dresden-Rossendorf, ***Germany.***

Outline

- Lattice structure
- Fermi surface
- Resistivity 122 Pn- and 122 Ch-
- TDO technique
- Magnetic penetration depth
- $H_{c2}(T)$ 122 pnictides
- $H_{c2}(T)$ 122 chalcogenides
- Summary

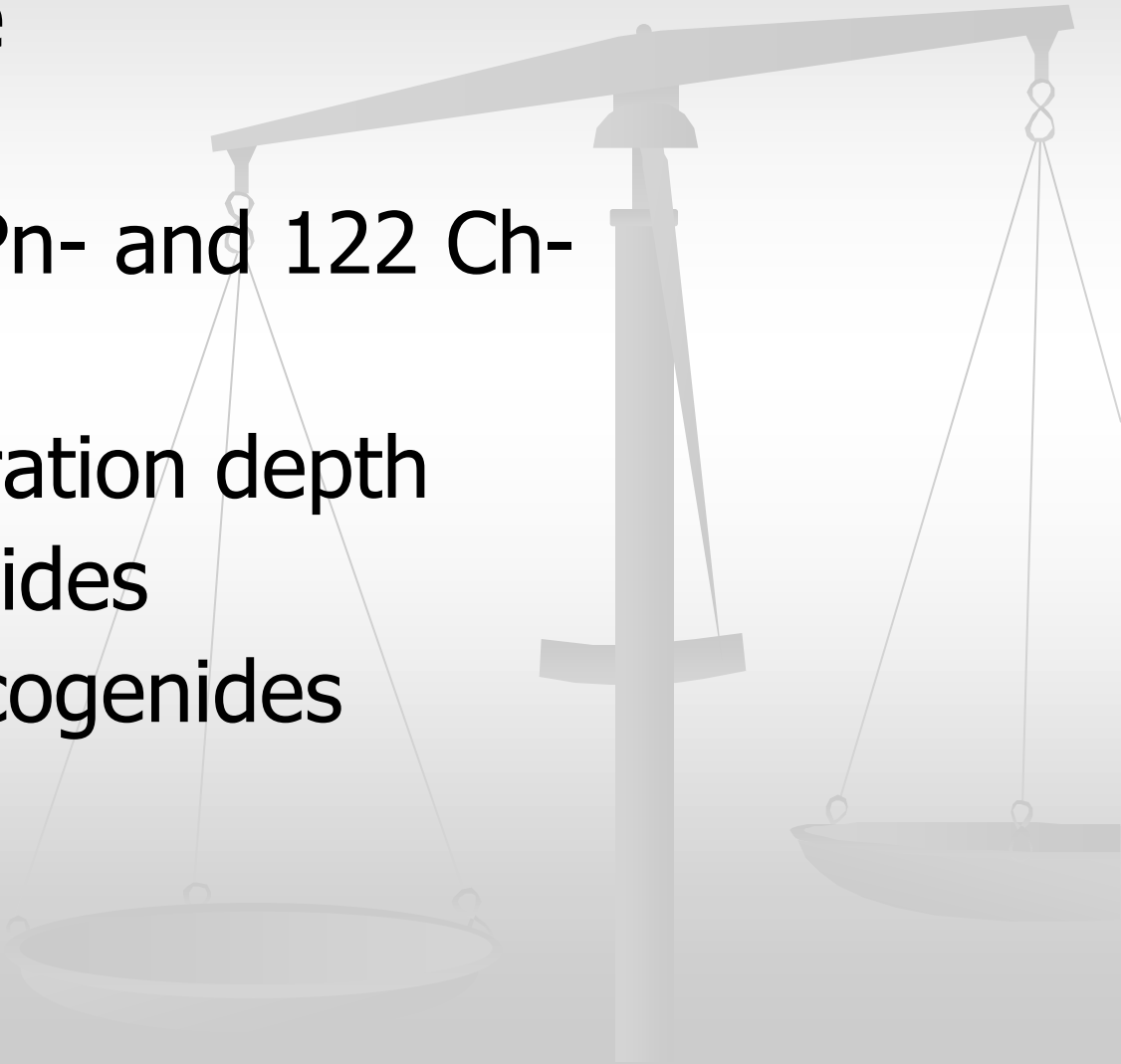

Crystal structure of $Eu_xBa_{1-x}Fe_2As_2$ (122)

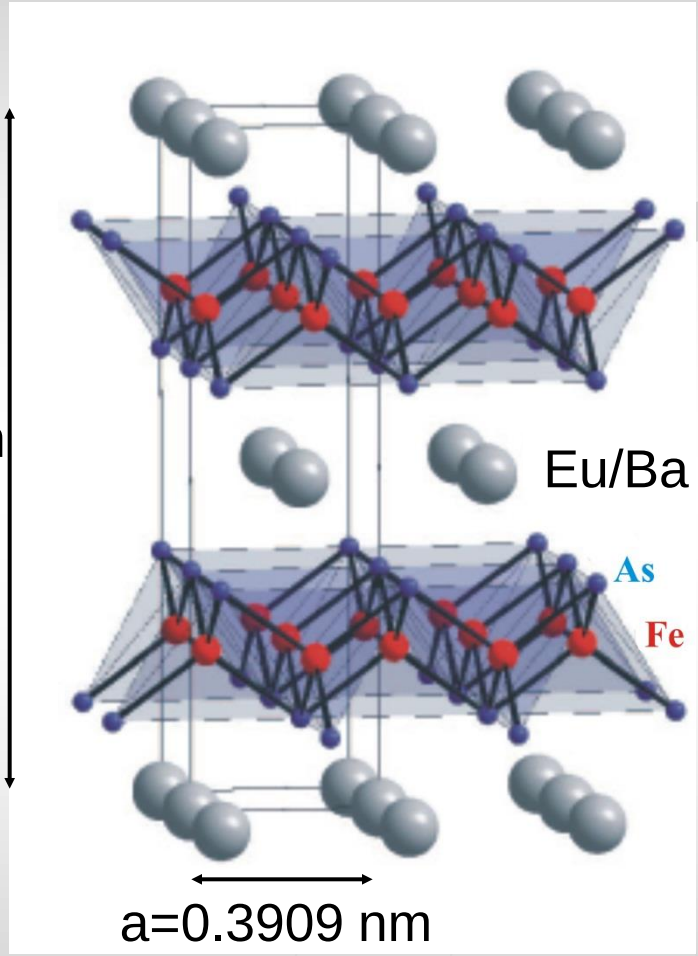

$Eu_{0.5}Ba_{0.5}Fe_2As_2$ $T_c \leq 32$ K

Crystal structure of KFe_2Se_2

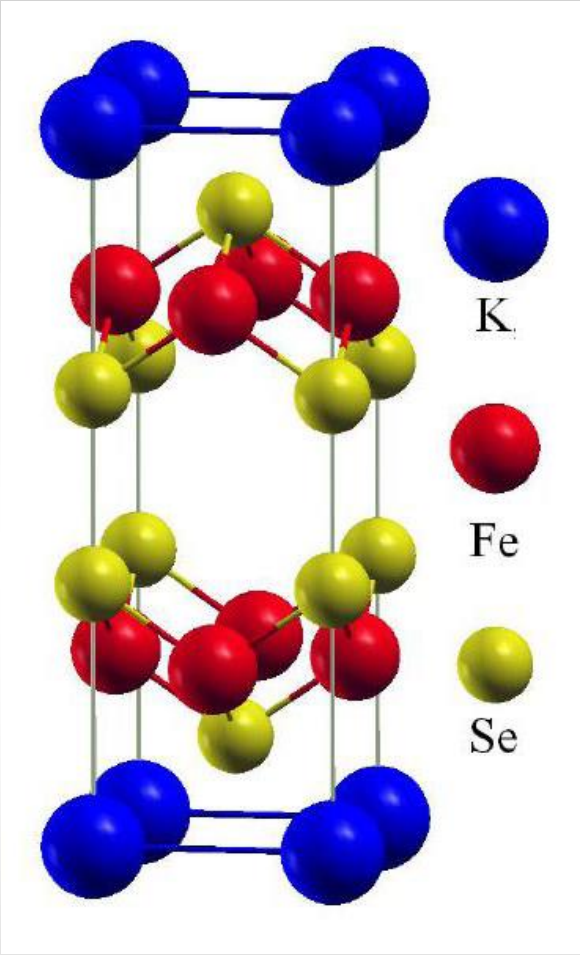

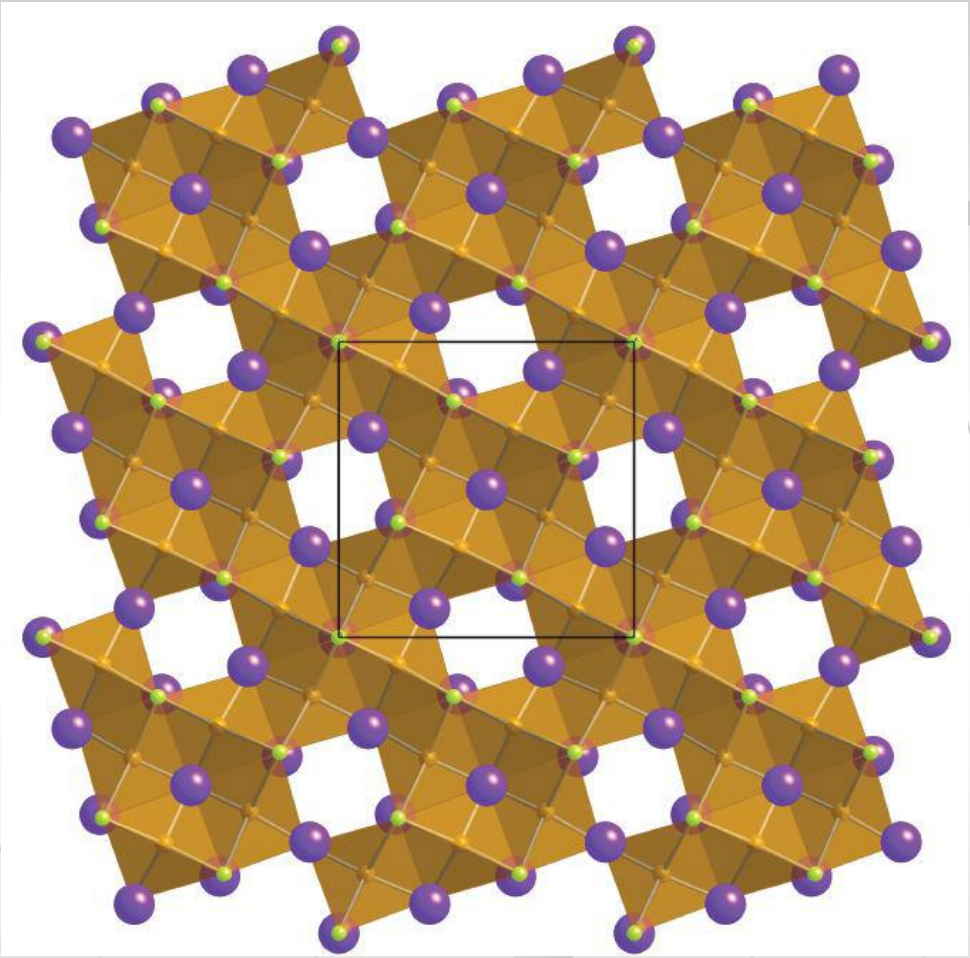

The superstructure of $K_{0.774}Fe_{1.61}Se_2$ from the [001] direction in the $\sqrt{5} \times \sqrt{5} \times 1$ supercell: fully occupied Fe sites decorated with ordered vacancy sites.
P. Zavalij et al., **ArXiv:1101.4882 (2011).**

Fermi surface of $K_xBa_{1-x}Fe_2As_2$ from ARPES

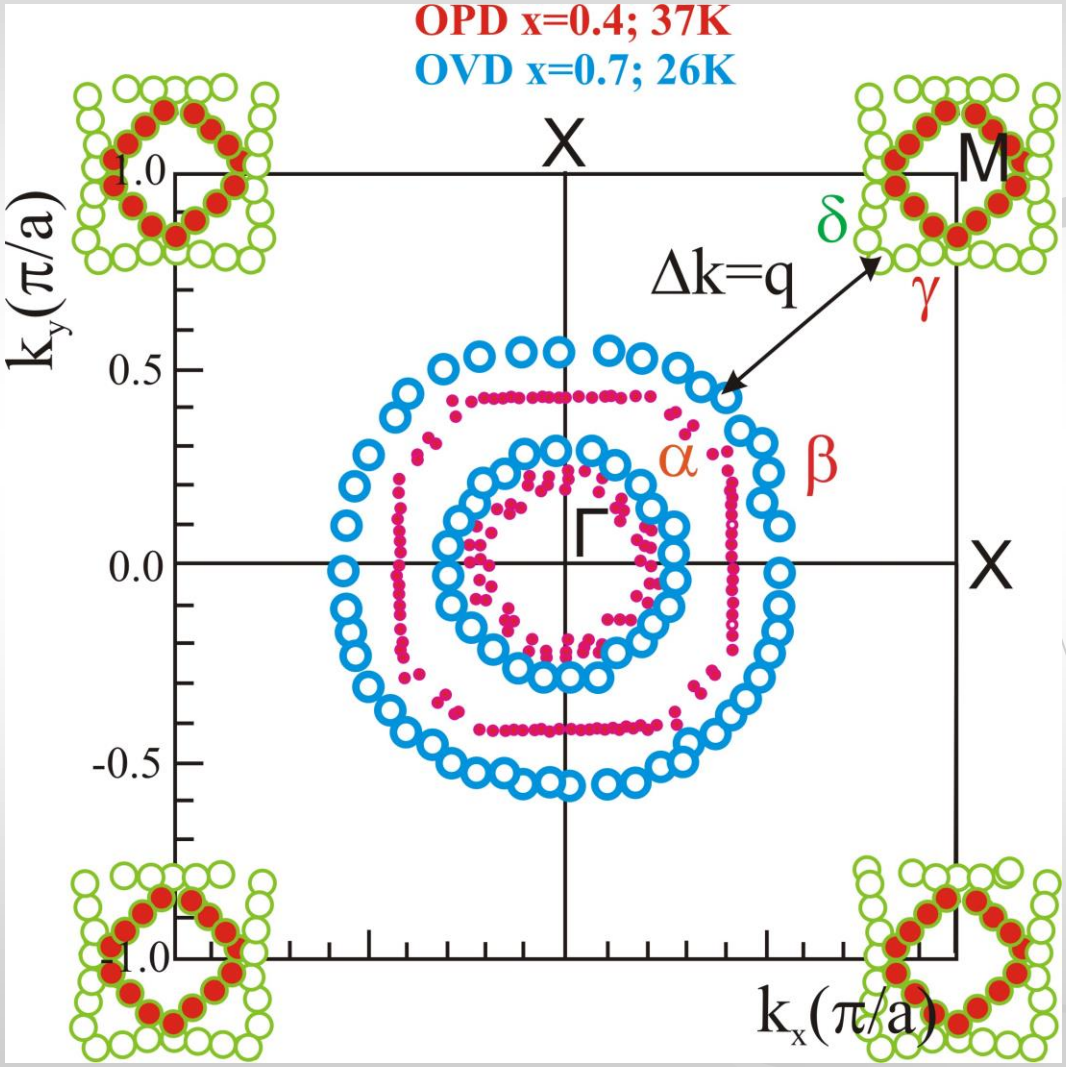

$T_0 = \hbar \Delta k s / k_B$ –
the temperature at which the phonon wave- vector *q* is equal to the inter-sheet distance *Δk*.
The effective masses:
$m^*_{0.4} = 4.8\ m_0$, $m^*_{0.7} = 9.0\ m_0$,
$m^*_{0.4} = m^*_{0.7} = 1.3\ m_0$

Schematic ARPES diagram summarizing the electronic band structure of $K_{0.8}Fe_{1.7}Se_2$

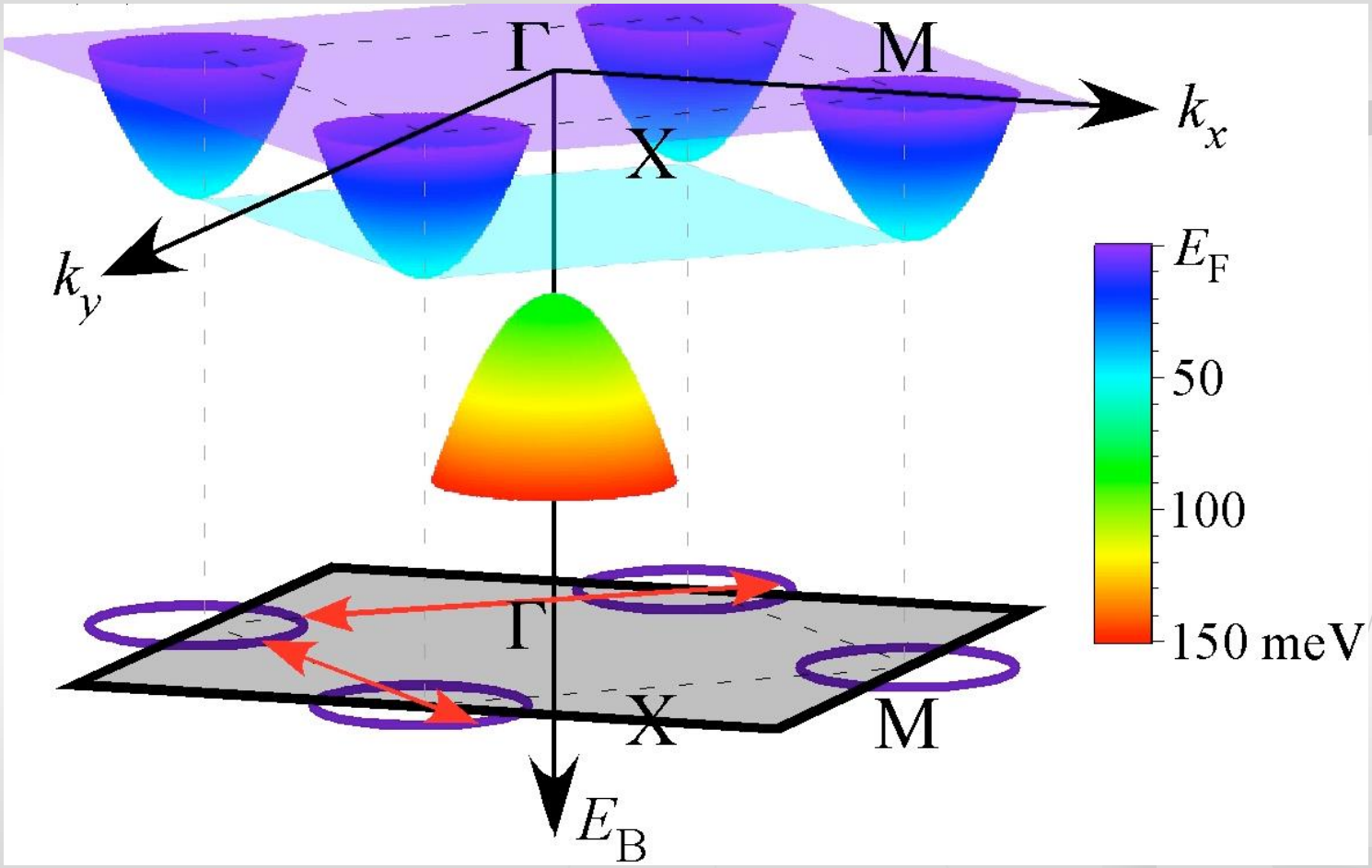

T. Qian et al., **arXiv:1012.6017**.

$Ba_{0.32}K_{0.68}Fe_2As_2$

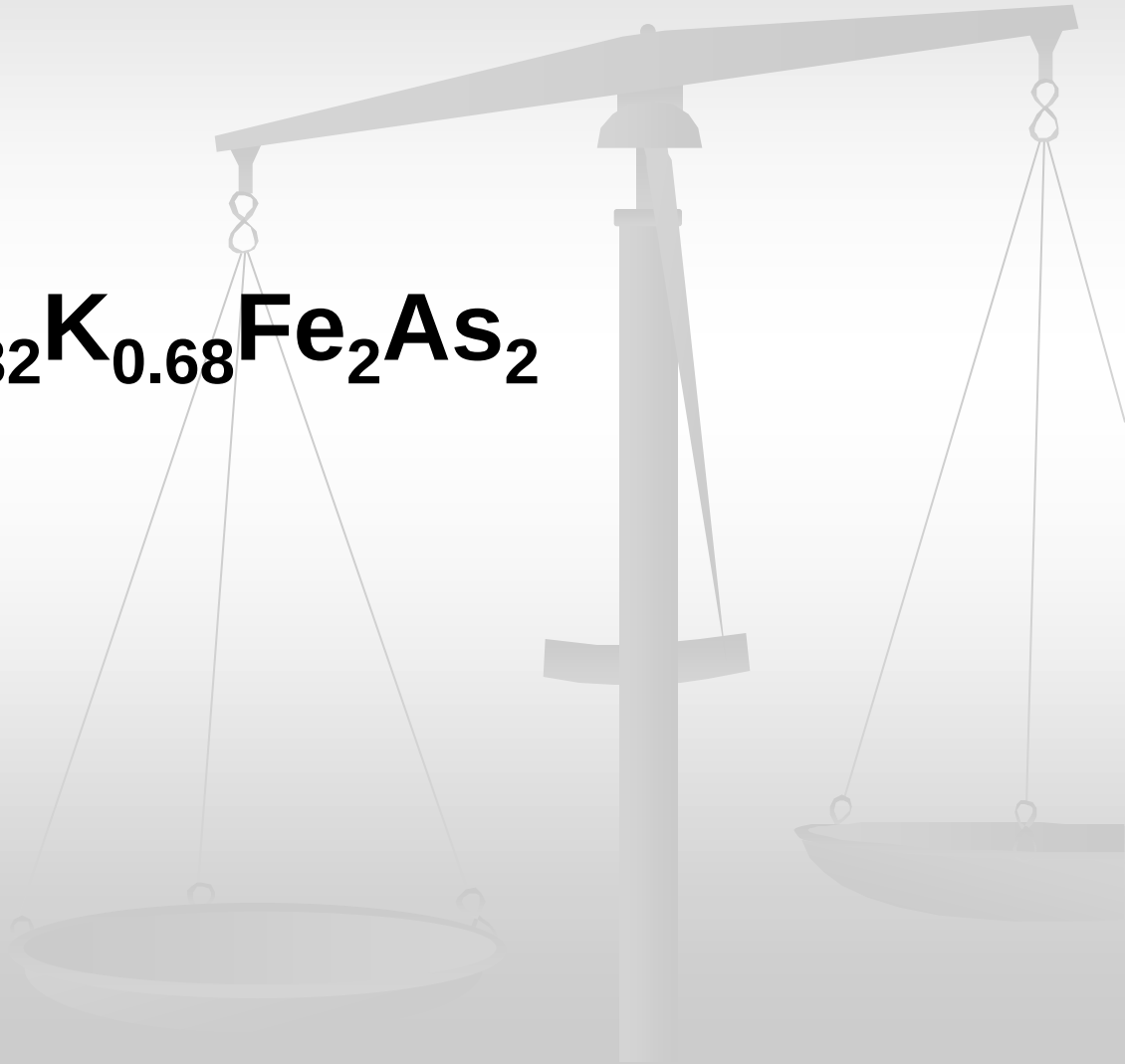

Temperature dependence of the $\rho_{ab}(T)$, of $K_{0.5}Ba_{0.5}Fe_2As_2$ and $K_{0.38}Ba_{0.62}Fe_2As_2$ single crystals in zero magnetic field.

Inter-sheet umklapp e-p scattering

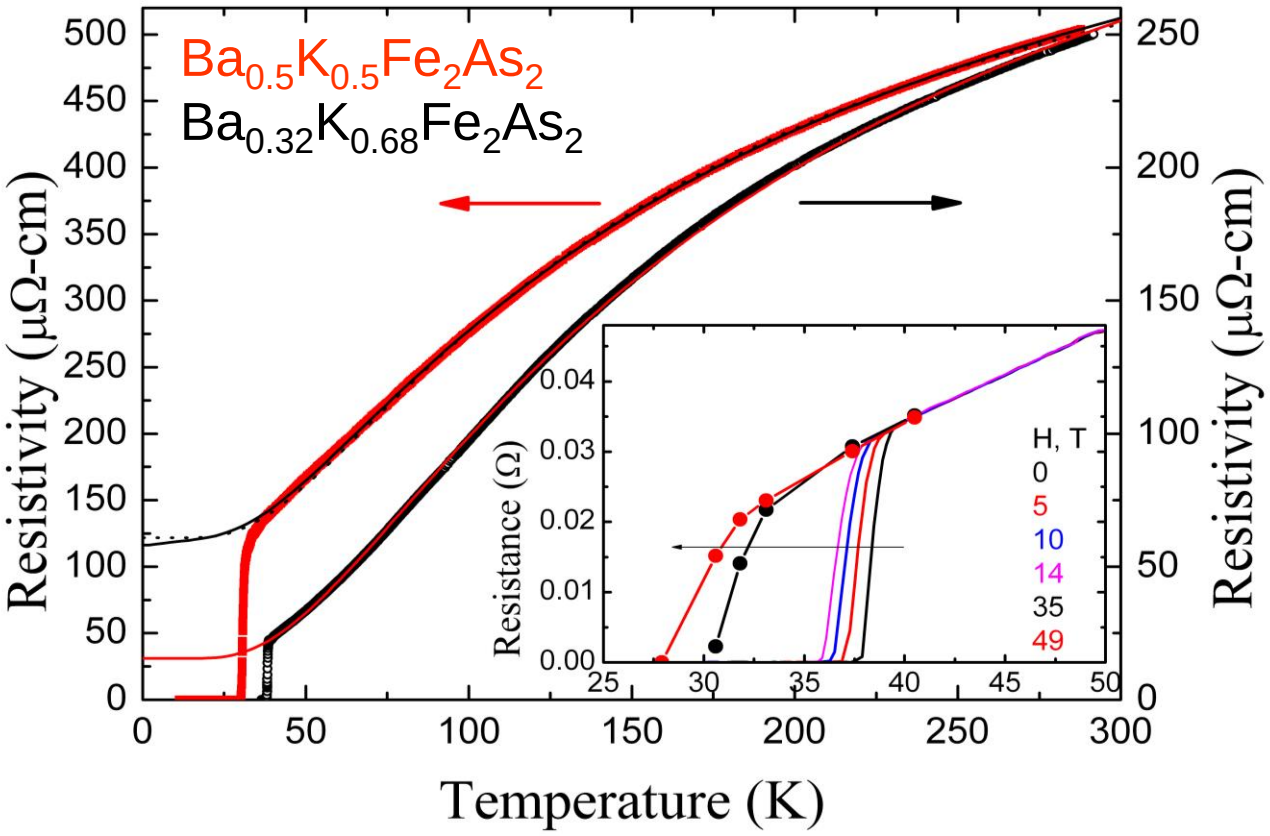

Dependence $\rho_{ab}(T)$ in $K_{0.32}Ba_{0.68}Fe_2As_2$
$\rho(0)$=15.5μΩcm,
ρ_1=0, C = 406μΩcm,
T_0=158K,
and $Ba_{0.5}K_{0.5}Fe_2As_2$
$\rho(0)$=115.3 μΩcm,
ρ_1=0.49 μΩcm,
n = 0.83, C=531μΩcm,
T_0=134 K
and ρ_1=0 dotted curve

$$\rho(T) = \rho(0) + \rho_1 T^n + Ce^{-T_0/T}$$

H. Wilson, Proc. R. Soc. A, London **167**, 580 (1938).

V.A. Gasparov et al., JETP Letters, **93**, 26 (2011).

Electron transport properties of $Ba_{0.68}K_{0.32}Fe_2As_2$ under pressure up to 15 kbar

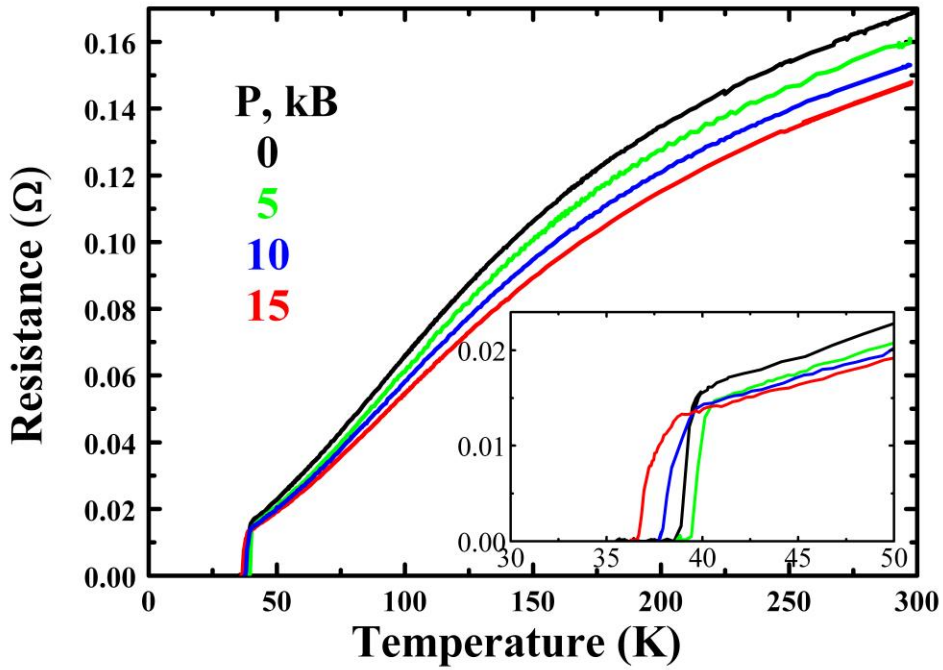

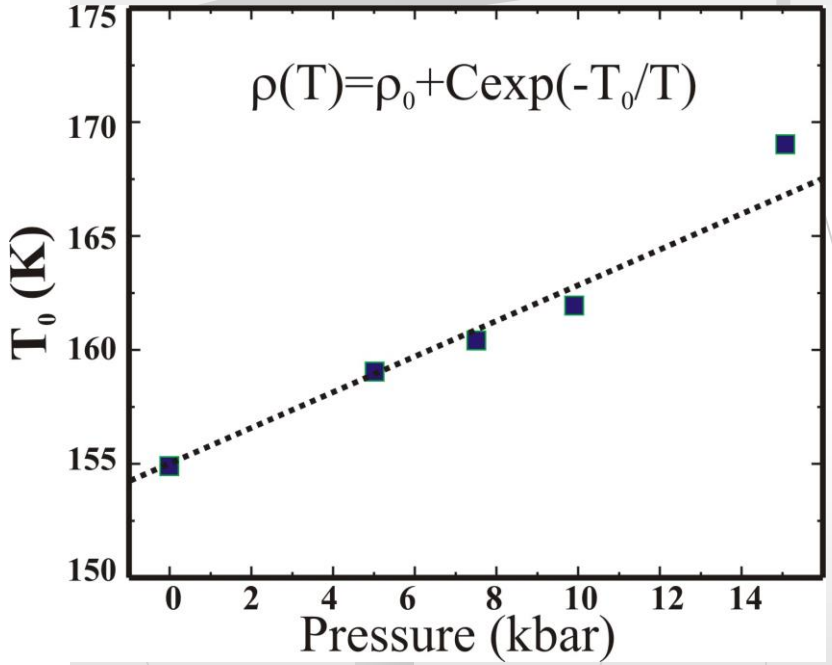

S. Arsenijevic *et al.*, to be published

Electron transport properties of $K_{0.8}Fe_{1.8}Se_2$

(a)

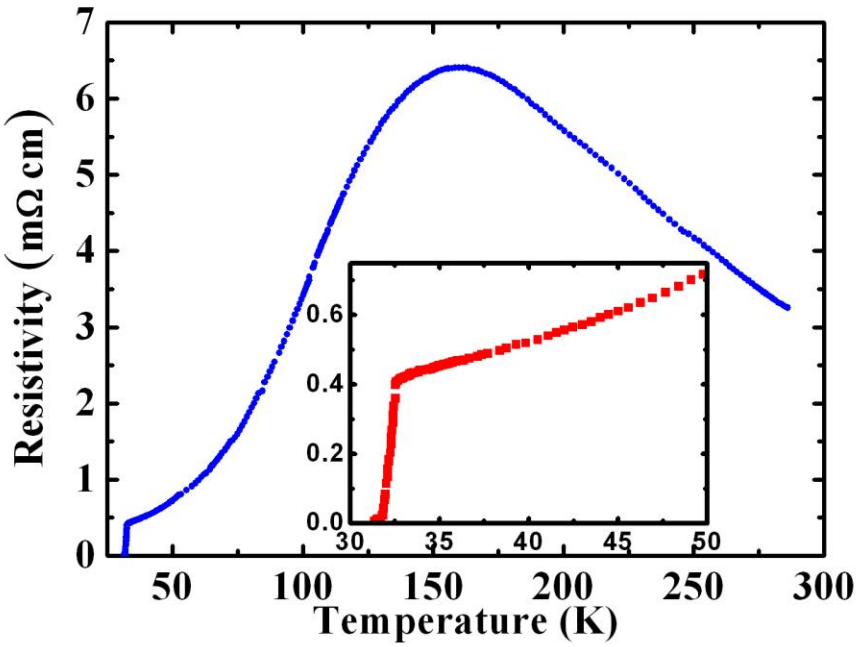

(b)

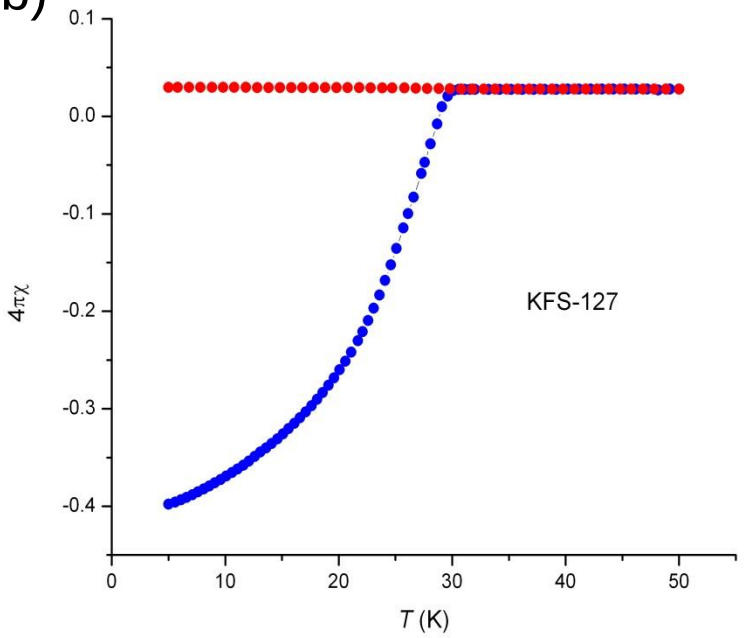

Temperature dependences of: (a) resistivity and (b) dc susceptibility

L. Li et al., Pys. Rev. B **84**, 174501 (2011).

Electron spin resonance in $K_xFe_{2-y}Se_2$

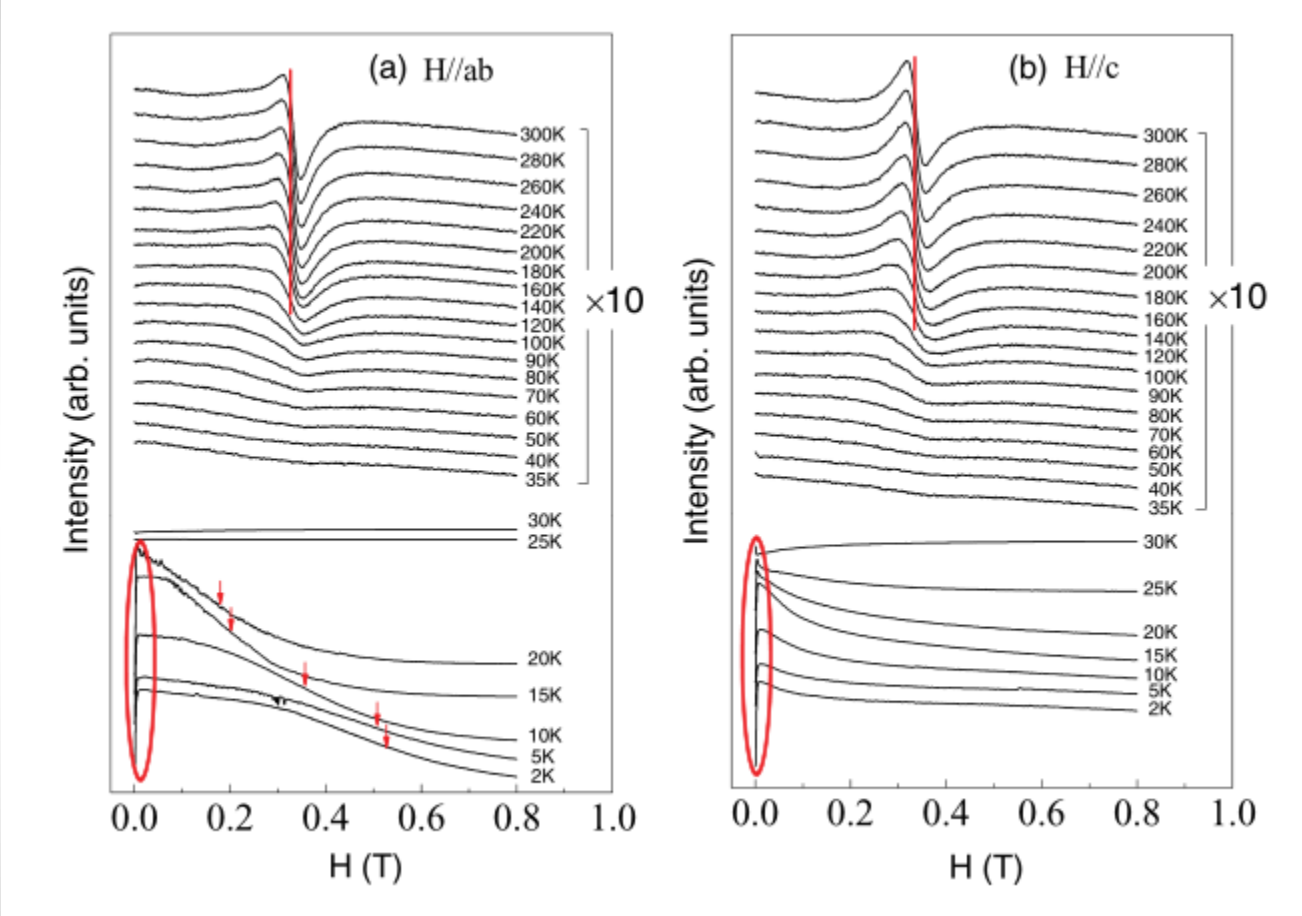

ESR spectra at different T for $K_xFe_{2-y}Se_2$ crystal with H// ab-plane and c-axis, respectively. The intensity of the spectrum between 40 K and 300 K has been multiplied by 10. The superconducting - feature spectrum is marked by a red ellipse. Red arrow denotes the resonance field of the resonance-characteristic spectrum below T_c.

The TDO frequency, susceptibility and the resistance of (a) $Ba_{0.68}K_{0.32}Fe_2As_2$ and (b) $Ba(Fe_{0.93}Co_{0.07})_2As_2$ close to T_c.

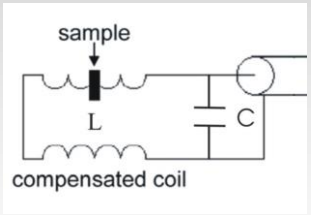

ТДО

(a)

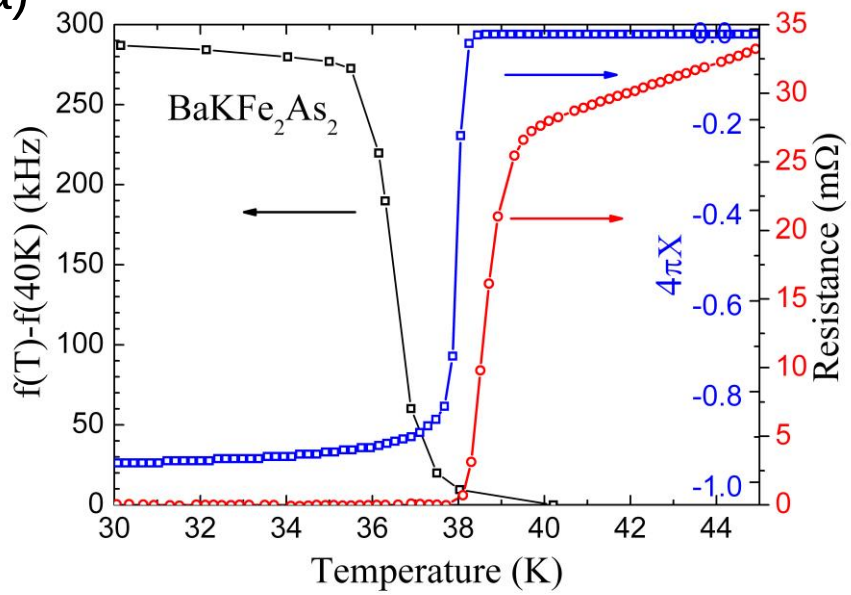

(b)

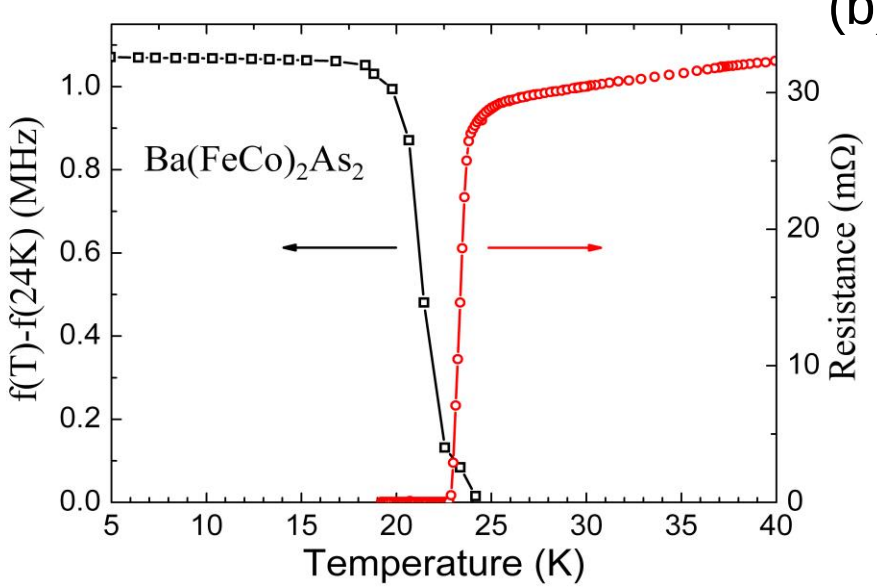

Temperature dependences of: **TDO frequency**, **resistivity** and **dc susceptibility**

V.A. Gasparov et al., JETP Letters, **93**, 667 (2011)

Experimental setup for $K_{0.8}Fe_2Se_2$

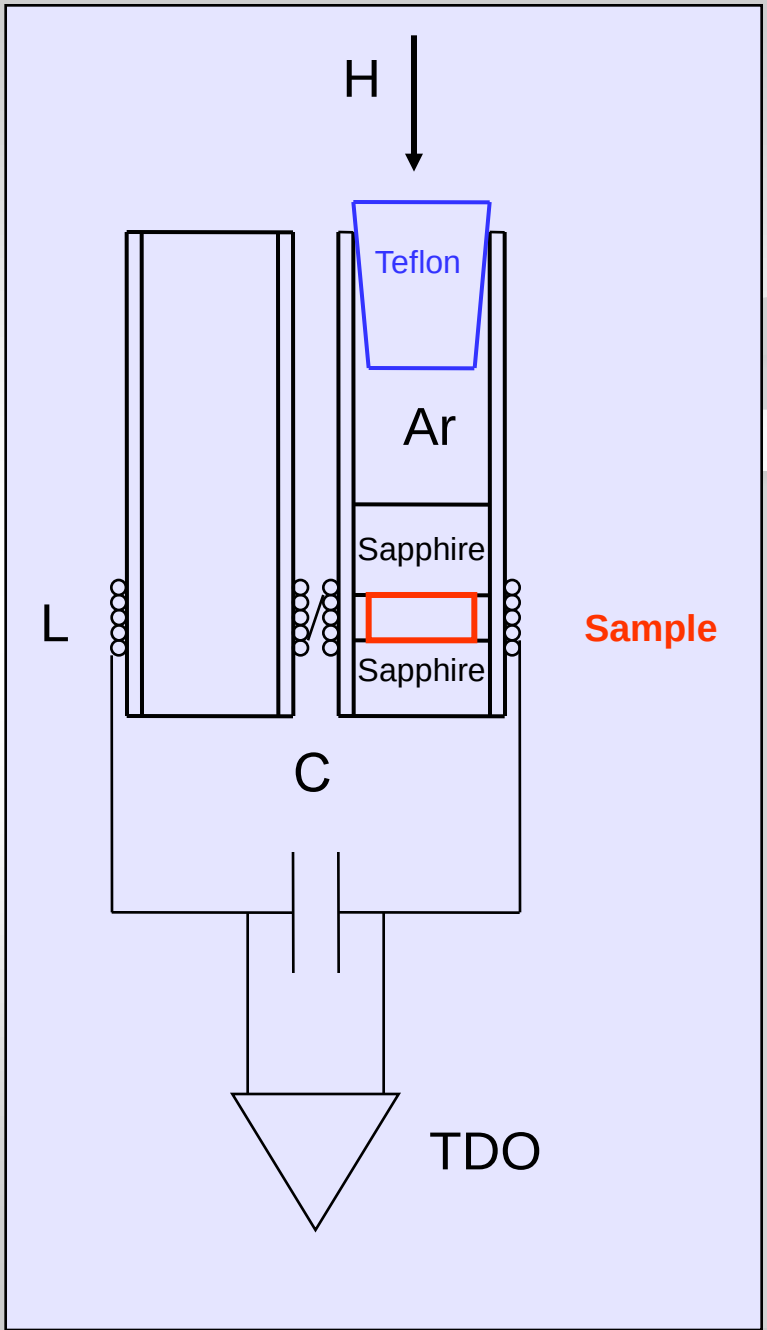

Field dependences of the TDO frequency shifts for $Eu_{0.5}K_{0.5}Fe_2As_2$ single crystal

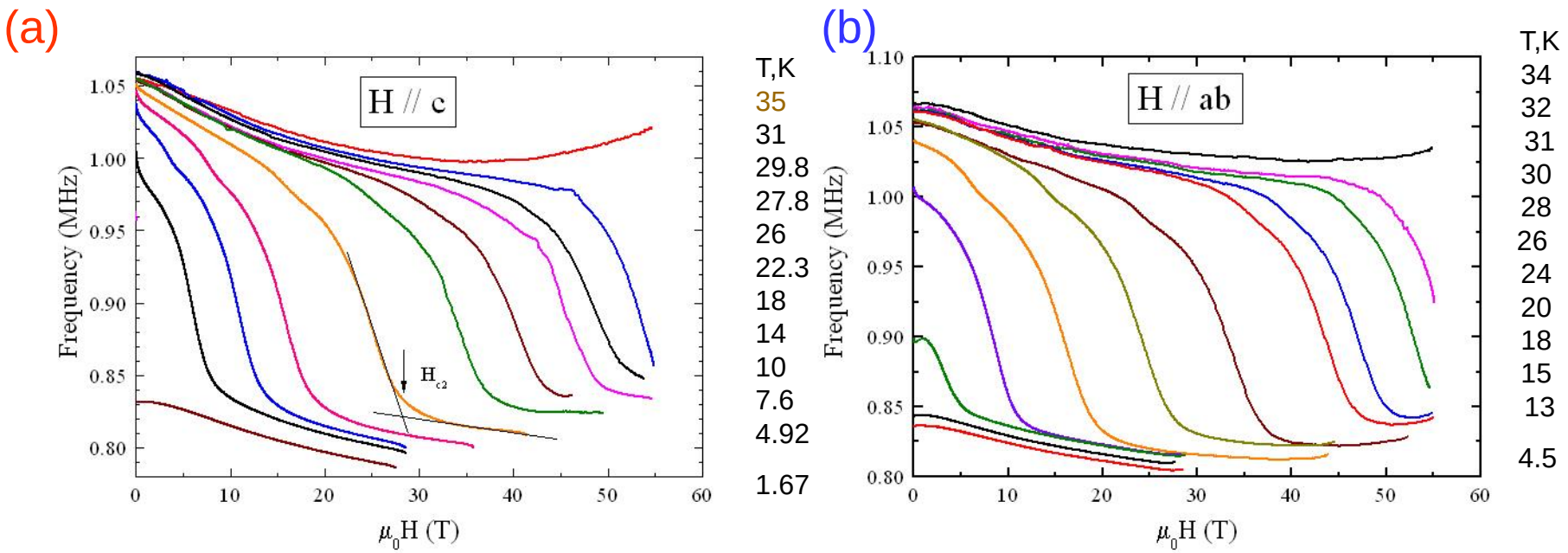

(a) Magnetic fields applied along the *c* direction and (b) H//*ab* direction

V.A. Gasparov et al., PRB **87**, 094508 (2013)

Field dependences of the TDO frequency shifts for $Ba(Fe_{0.93}Co_{0.07})_2As_2$ single crystal

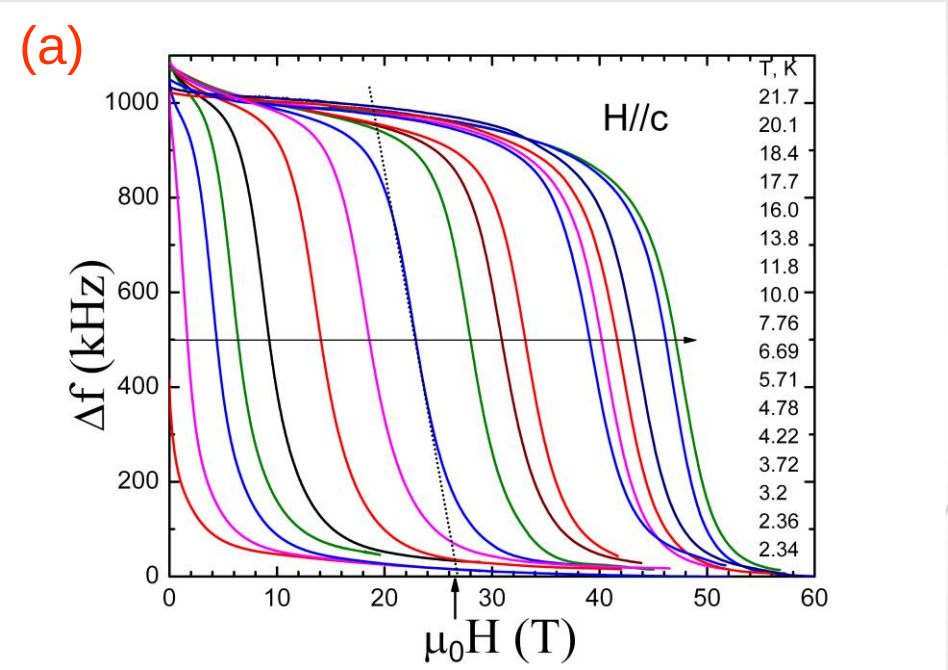

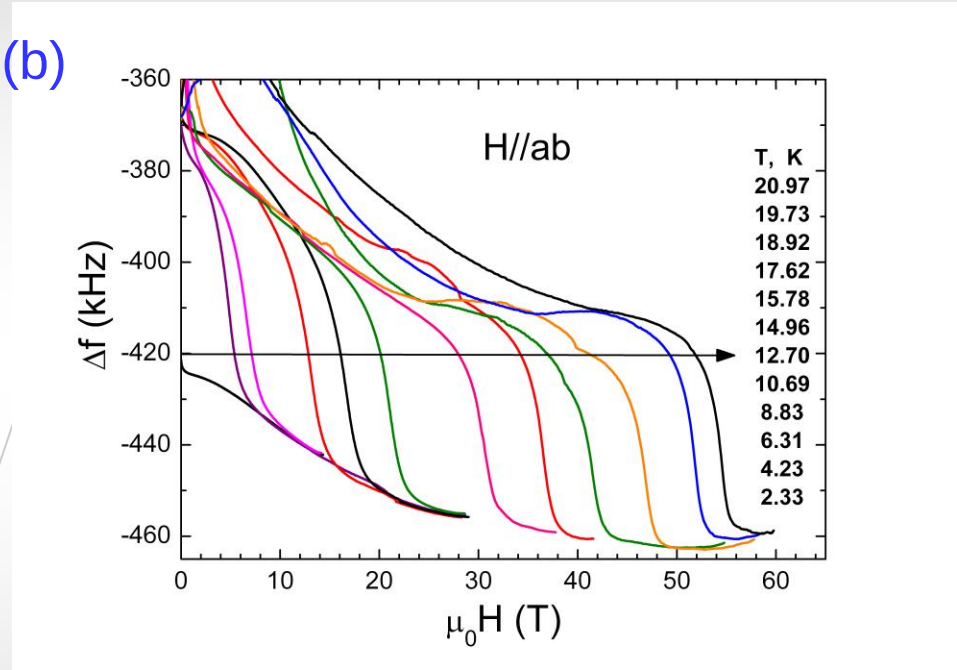

Field dependences of the TDO frequency shifts for $Ba(Fe_{0.93}Co_{0.07})_2As_2$ for magnetic fields applied (a) along the c direction and (b) parallel to the ab plane.

V.A. Gasparov et al., JETP Letters, **93**, 667 (2011)

$K_{0.8}Fe_2Se_2$

Field dependences of the TDO frequency shifts for $K_{0.8}Fe_2Se_2$ single crystal

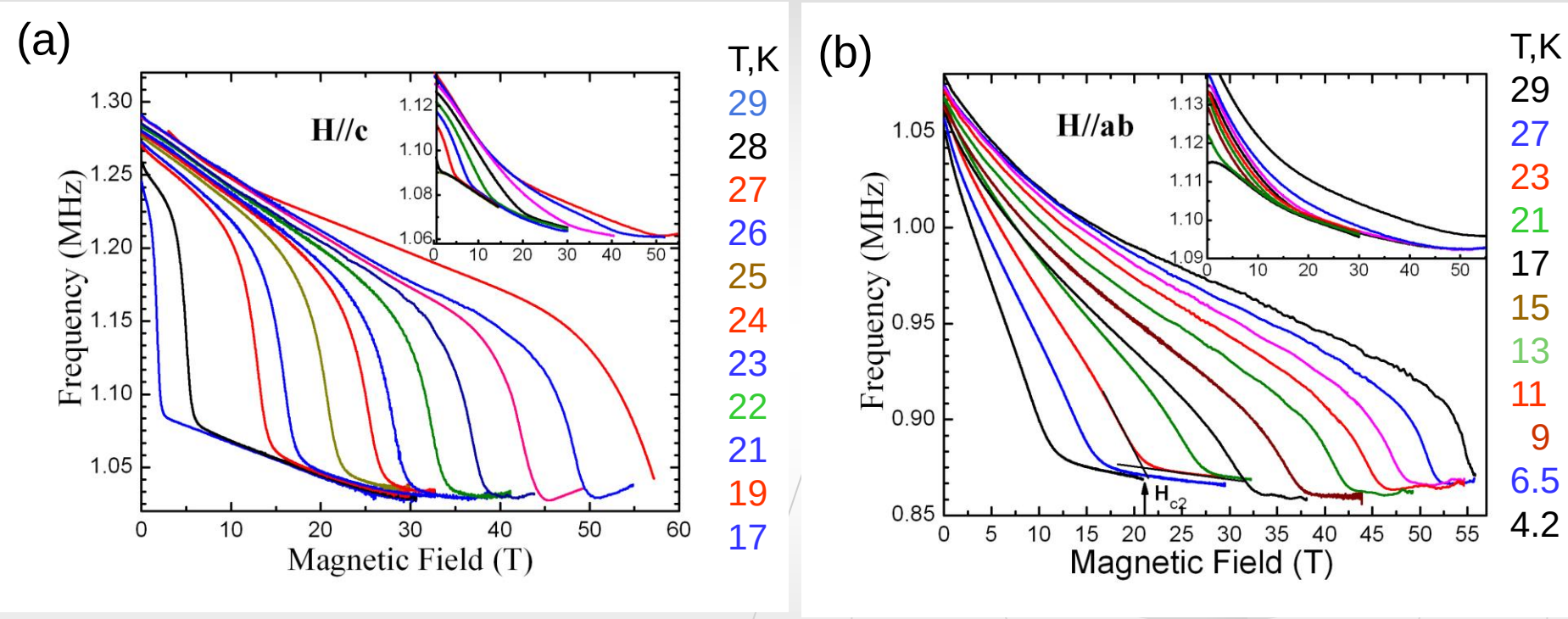

Field dependences of the TDO frequency shifts for $K_{0.8}Fe_2Se_2$ for magnetic fields applied: (a) along the c direction and (b) a,b direction. Inset – similar data for $K_{0.83}Fe_{1.83}Se_2$.

V.A. Gasparov et al., PRB **87**, 094508 (2013)

$Rb_{0.8}Fe_2Se_2$

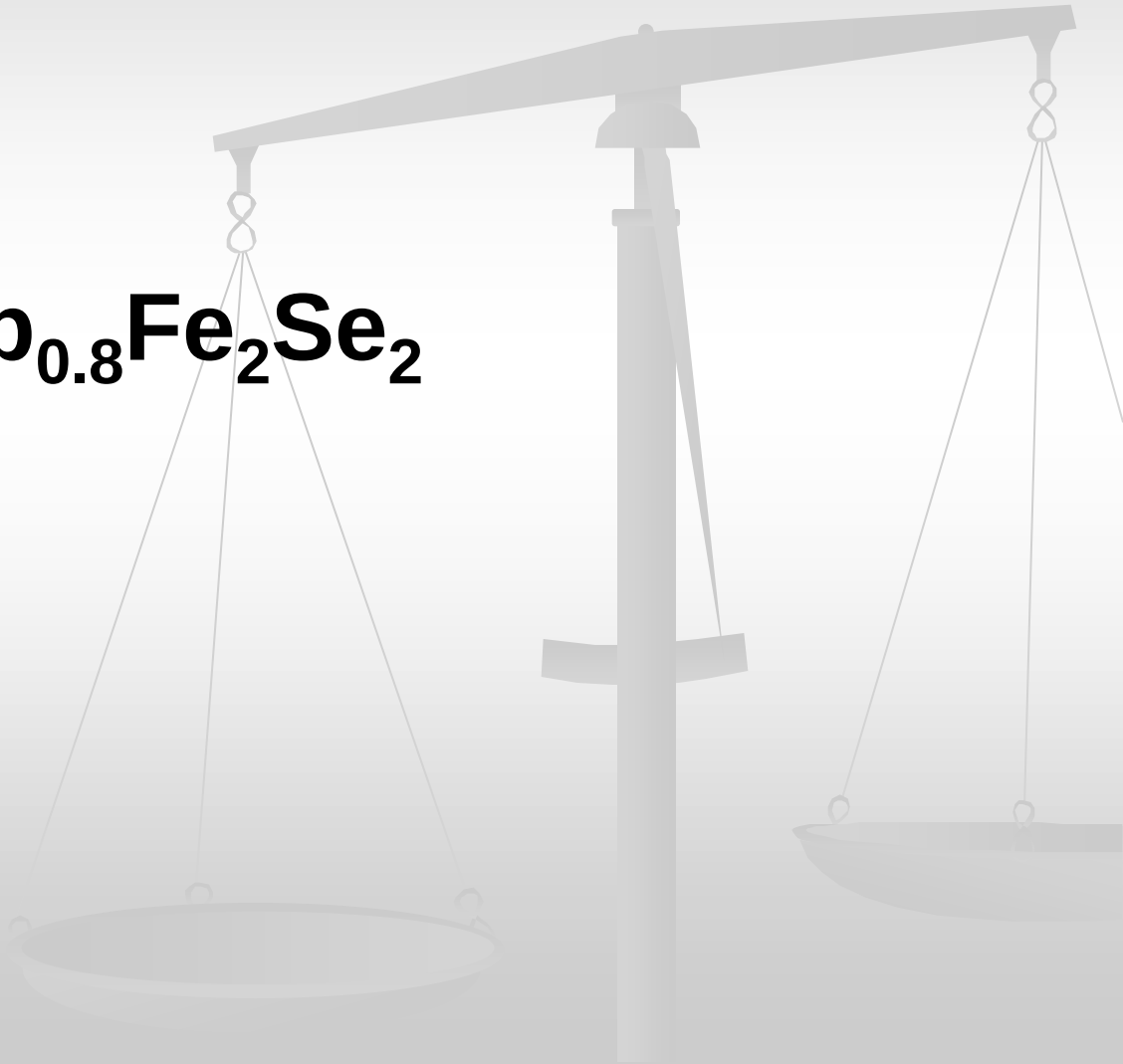

Temperature dependence of magnetic penetration depth in $Rb_{0.8}Fe_2Se_2$ single crystal

(a)

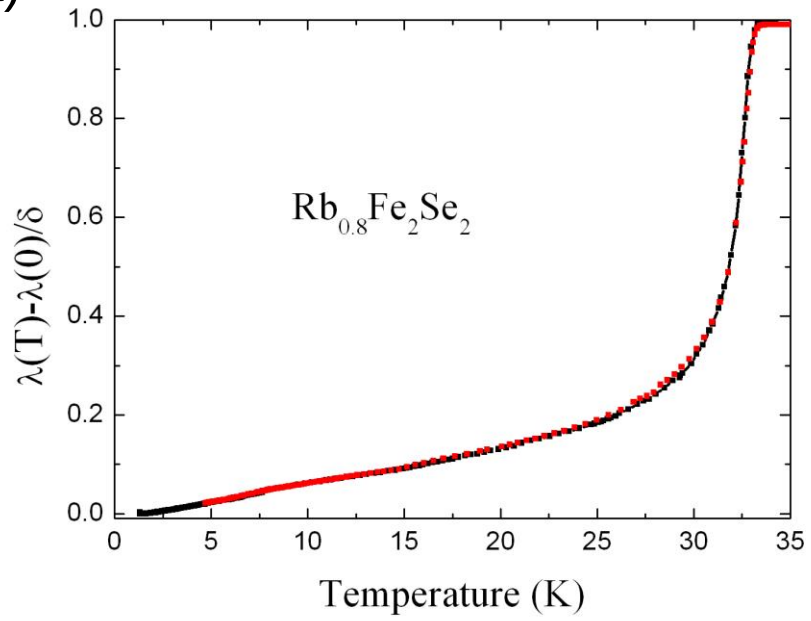

(b)

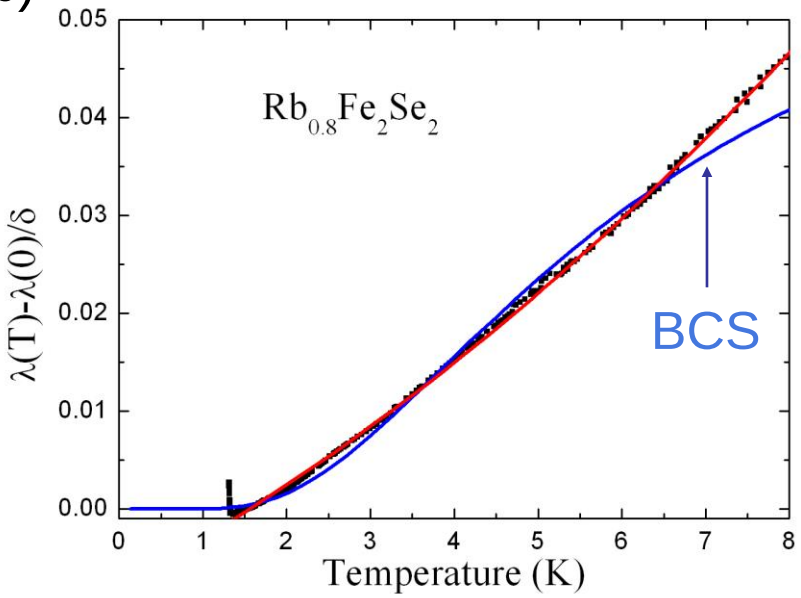

(a) $T<T_c$; (b) $T<T_c/4$

BCS:

$$\frac{\lambda(T)-\lambda(T_1)}{\delta}=\frac{\lambda(0}{\delta}\times[\sqrt{\frac{\pi\Delta(0)}{2k_BT}}\times\exp(-\frac{\Delta(0)}{k_BT})-\sqrt{\frac{\pi\Delta(0)}{2k_BT_1}}\times\exp(-\frac{\Delta(0)}{k_BT_1})]$$

Temperature dependence of $H_{c2}(T)$

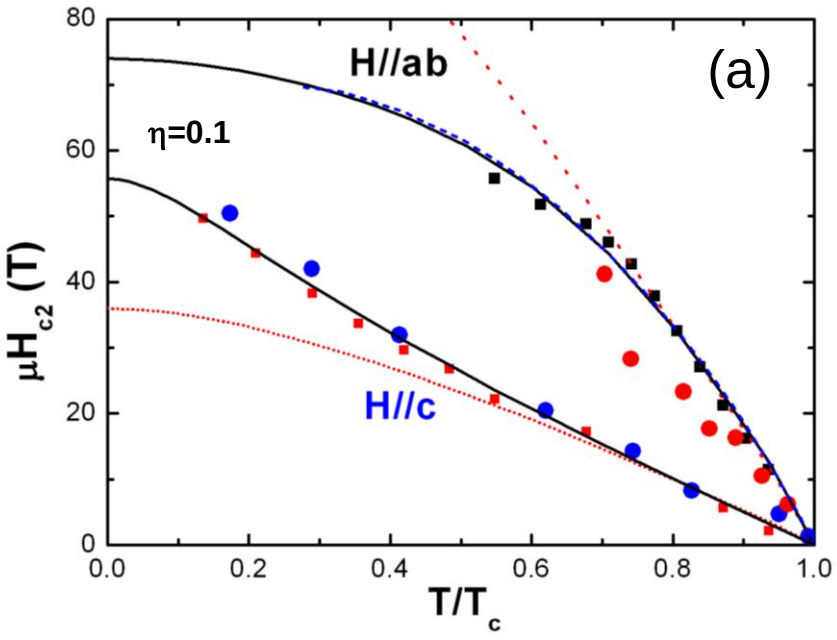

$K_{0.8}Fe_2Se_2$

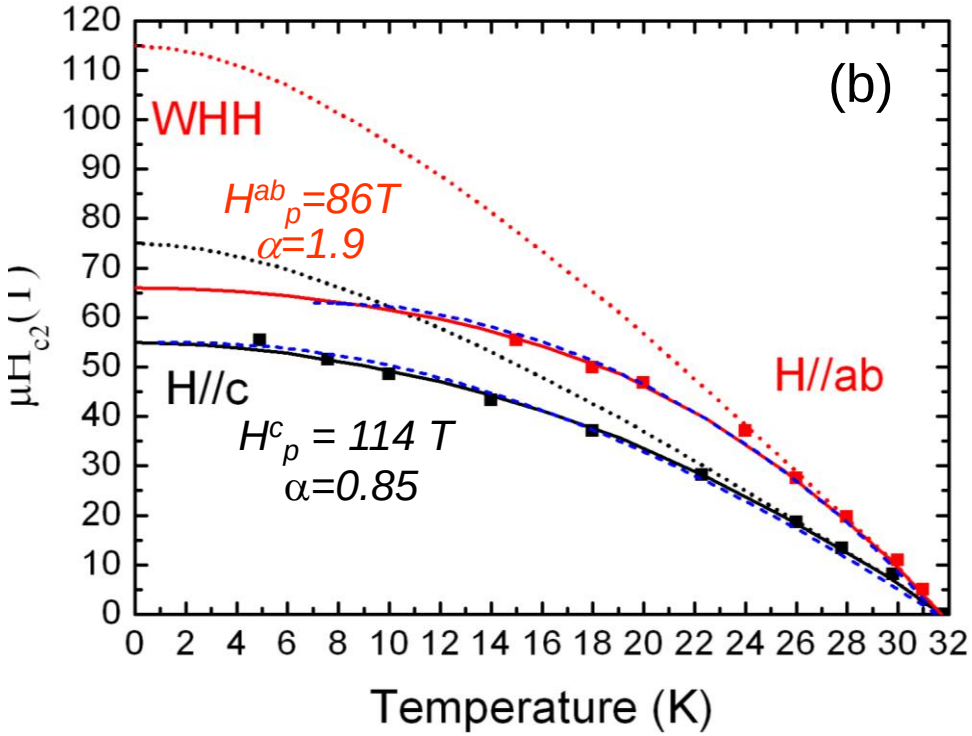

$Eu_{0.5}K_{0.5}Fe_2As_2$

Temperature dependences of the $H_{c2}(T)$, for (a) $K_{0.83}Fe_{1.83}Se_2$ (red circles), $K_{0.8}Fe_2Se_2$ (squares) and (b) $Eu_{0.5}K_{0.5}Fe_2As_2$ for $H \parallel c$ and $H \parallel ab$. The lines show the dependencies including Pauli pair breaking: solid one with α(T) and dashed - α=const. The solid curve in (a) for H//c is a two band fit with $\eta = D_2/D_1 = 1.0$. The dotted lines indicate the temperature dependences according to the WHH model.

We obtain $\xi^{ab}(0) = \sqrt{\phi_0 / 2\pi H^{*c}{}_{c2}} = 2.83nm$ and $\xi^{c}(0) = \phi_0 / 2\pi\xi^{ab} H^{*ab}{}_{c2} = 1.2nm$ for $K_{0.8}Fe_2Se_2$, and $\xi_{ab}(0)$ = 2.1 nm and $\xi_c(0)$ = 1.36 nm for $Eu_{0.5}K_{0.5}Fe_2As_2$

V.A. Gasparov et al., PRB **87**, 094508 (2013)

Orbital and spin pair breaking in $H_{c2}(T)$

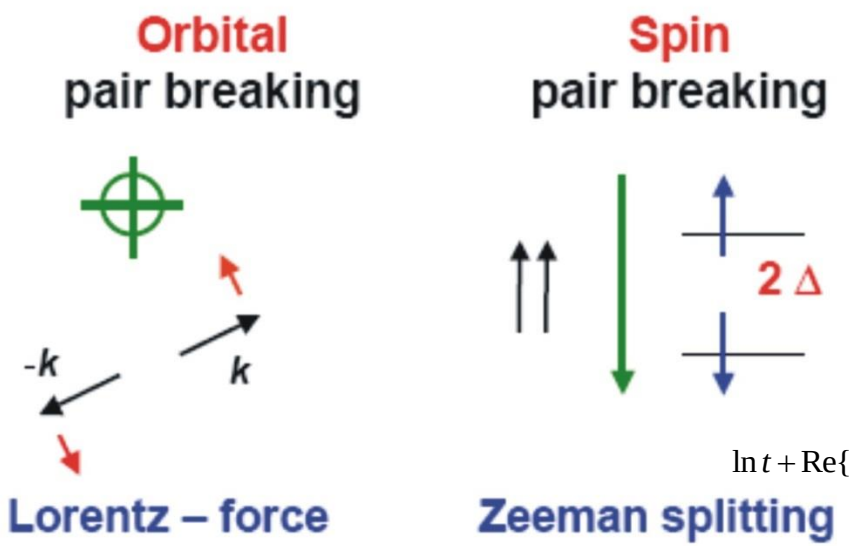

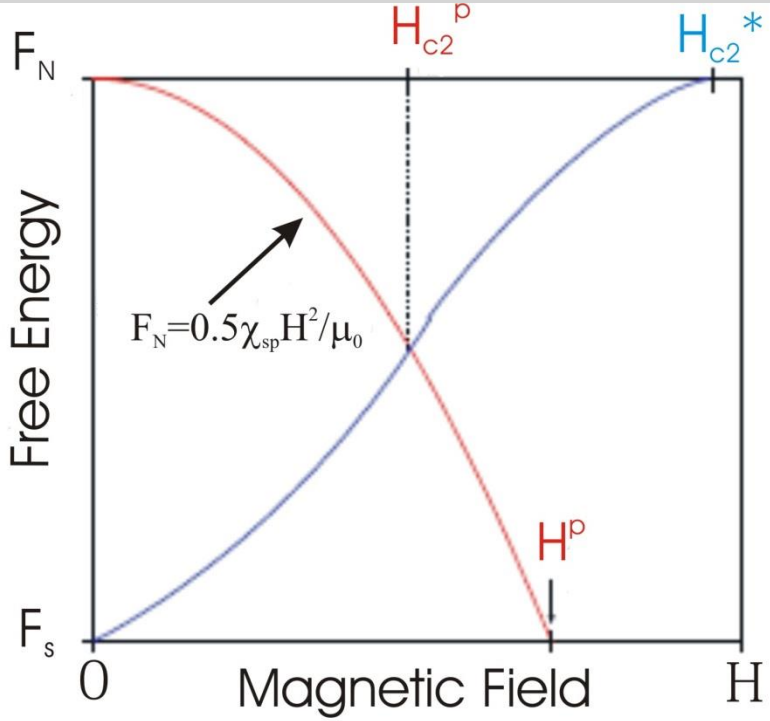

Werthamer–Helfand–Hohenberg orbital model:
$H^*_{c2}(0) \approx -0.69 T_c \, (dH_{c2}/dT) \, |T_c$
Pauli spin model: $H_{c2}(T) = H^*_{c2}(T)/[1 + \alpha^2]^{1/2}$

$\alpha = \sqrt{2}\, H^*_{c2}(0)/H_p(0)$ - parameter Maki; Fuchs - $\alpha = \sqrt{2}\, H^*_{c2}(T)/H_p(0)$

$$\ln t + \mathrm{Re}\{\psi[0.5 + 0.138\frac{h}{t}(1 + i\alpha)] - \psi(0.5)\} = 0$$

$t=T/T_c$; $h=H_p(T)/H^*_{c2}(0)$

$H^c_p = 114T$ ($\alpha = 0.85$) and $H^{ab}_p = 86T$ ($\alpha = 1.9$), for $H \parallel ab$ and $H \parallel c$

Two gap Gurevich model of $H_{c2}(T)$

$$H_{c2}(0) = \frac{\phi_0 k_B T_c}{1.12\hbar\sqrt{D_1 D_2}} \exp(\frac{g}{2})$$

g – complicated function of the matrix:

$\lambda_{mm'} = \lambda^{(ep)}_{mm'} - \mu_{mm'}$

$\mu_{mm'}$ the matrix of the Coulomb pseudopotential

$\lambda^{(ep)}_{mm'}$ electron–phonon coupling constants

at $\lambda_{12} = \lambda_{21} = \lambda_{22} = \lambda_{11} = 0.5$, $H_{c2}(T)$ follows Usadel equation

$$2\ln t + U(h) + U(\eta h)] = 0$$

t=T/T_c; h = $H_{c2}D_1\hbar/2\phi_0 k_B T$;

U(x)= $\Psi(1/2+x) - \Psi(1/2)$; $\Psi(x)$ – *the digamma function;*

$\eta = D_2/D_1$; $D = lv/3$ – the electronic diffusivities

$$D_1 \approx \frac{8\phi_0 k_B}{\pi^2 \hbar \mathrm{dH_{c2}/dT}} = 1.22\ \mathrm{cm^2/sec},\ \ \mathrm{D_2} = 0.12\mathrm{cm^2/sec}$$

CONCLUSION

- We find that $\rho(T)$ of 122 superconductors is due to intersheet umklapp electron-phonon scattering between light electrons to heavy hole sheets.
- We find that the resistivity of $K_{0.83}Fe_{1.83}Se_2$ in zero field may have AF transition.
- We studied $H_{c2}(T)$ in single crystals of hole- $(Ee_{0.5}K_{0.5}Fe_2As_2)$ and electron-doped: $K_{0.8}Fe_2Se_2$ superconductors in pulsed magnetic fields up to **57T**.
- For hole-doped $Ee_{0.5}K_{0.5}Fe_2As_2$, we can account for the temperature dependence of $H_{c2}(T)$ with slightly different fitting parameters, namely, the Pauli-limiting field $H^c_p = 114\ T$ and $H^{ab}_p = 86T$ for $H \parallel c$ and $H \parallel ab$, respectively.
- For electron-doped KFS, the data support a a single gap Pauli scenario for $H \parallel ab$ too.
- At the same time, $H_{c2}(T)$ for $K_{0.8}Fe_2Se_2$ at **H//c** is due to two gap model with one order difference of the diffusivities for different sheets of the FS.
- We obtained three times different coherence length: $\xi^{ab}(0) = 2.83\ nm$ versus $\xi^{c}(0) = 1.2\ nm$ for $K_{0.8}Fe_2Se_2$ and $\xi^{ab}(0) = 2.1\ nm$ versus $\xi^{c}(0) = 1.36\ nm$ for $Ee_{0.5}K_{0.5}Fe_2As_2$. These estimations are larger then the thickness of superconducting layers: 0.32 nm → 3D superconductivity.